JOURNAL OF PROPULSION AND POWER
Vol. 9, No. 1, Jan.–Feb. 1993

Thrust Vectoring: Theory, Laboratory, and Flight Tests

Benjamin Gal-Or,* and Valery Sherbaum†
Technion—Israel Institute of Technology, Haifa 32000, Israel

Fundamental concepts of vectored propulsion are defined and represented by novel designs of thrust-vectoring (TV) nozzles for maximized post-stall (PST)-agility. The concepts are employed to formulate a unified mathematical phenomenology for PST vectored fighter aircraft. The phenomenology is combined with an unorthodox methodology to test alternative prototypes of agile tailless vectored fighters and the efficiency of upgraded (conventional) fighters. Two PST-TV control rules have also been formulated.

Nomenclature

b = reference span, m
C_D = drag coefficient, dimensionless
C_{DS} = nozzle discharge coefficient, dimensionless
C_{fg} = engine nozzle thrust coefficient, dimensionless, [cf. Eqs. (16–18)]
CG = center of gravity, percentage mean aerodynamic chord
C_L = lift coefficient, dimensionless
C_l = rolling moment coefficient, dimensionless
$C_{l\beta}$ = rolling moment derivative with respect to sideslip angle, 1/rad
$C_{l\delta a}$ = aileron effectiveness derivative, 1/rad
$C_{l\delta e}$ = stabilator effectiveness derivative, 1/rad
$C_{l\delta\Delta e}$ = differential stabilator effectiveness derivative, 1/rad
$C_{l\delta r}$ = rudder effectiveness derivative (variation of rolling moment coefficient with respect to rudder angle), 1/rad
C_{lp} = roll damping derivative, 1/rad
C_{lr} = rolling moment derivative with respect to yaw rate, 1/rad
C_m = pitching moment coefficient, dimensionless
C_{mo} = basic pitching moment coefficient, dimensionless
C_{mq} = pitching moment derivative with respect to pitch rate, 1/rad
C_n = yawing moment coefficient, dimensionless
$C_{n\beta}$ = yawing moment derivative with respect to sideslip angle, 1/rad
$C_{n\beta^*}$ = yawing moment derivative high angle-of-attack increment with respect to sideslip angle, 1/rad
$C_{n\delta a}$ = yawing moment derivative with respect to aileron deflection, 1/rad
$C_{n\delta e}$ = yawing moment derivative with respect to stabilator deflection, 1/rad
$C_{n\delta\Delta e}$ = yawing moment derivative with respect to differential stabilator deflection, 1/rad
$C_{n\delta r}$ = rudder effectiveness derivative (variation of yawing moment coefficient with respect to rudder angle), 1/rad
C_{np} = yawing moment derivative with respect to roll rate, 1/rad
C_{nr} = yaw damping derivative, 1/rad
C_{py} = side c.p. (for PSM in the y-direction)
C_x = longitudinal force coefficient, dimensionless
C_y = side force coefficient, dimensionless
$C_{y\beta}$ = side force derivative with respect to sideslip angle, 1/rad
$C_{y\beta^*}$ = asymmetric side force derivative high angle-of-attack increment with respect to sideslip angle, 1/rad
$C_{y\delta a}$ = side force derivative with respect to aileron deflection, 1/rad
$C_{y\delta e}$ = side force derivative with respect to stabilator deflection, 1/rad
$C_{y\Delta e}$ = side force derivative with respect to differential stabilator deflection, 1/rad
$C_{y\delta r}$ = side force derivative with respect to rudder deflection, 1/rad
C_{yp} = side force derivative with respect to roll rate, 1/rad
C_{yr} = side force derivative with respect to yaw rate, 1/rad
C_z = normal force coefficient, dimensionless
c = reference mean aerodynamic chord, m
D = the distance from TV nozzle exit to aircraft C_{py}, m
D^* = the distance from TV nozzle exit to aircraft CG, m
D_{cpy} = the drag operating @ C_{py}, kgf
G_z, G_y, G_x = g-onsets on the pilot in the respective body-axis coordinates, m/s²
g = gravitational constant, m/s²
I_x = moment of inertia about the roll axis, kg-m²
I_{xy} = cross product of inertia between roll and pitch axes, kg-m²
I_{xz} = cross product of inertia between roll and yaw axes, kg-m²
I_y = moment of inertia about the pitch axis, kg-m²
I_z = moment of inertia about the yaw axis, kg-m²
L = linear scale factor, dimensionless
LDC = local distortion coefficient lines at compressor inlet, $[(P_t - P_{tav})/P_{tav}) \times 10^{-3}]$, dimensionless
M = vehicle mass, kg; also Mach number (dimensionless)
M = nozzle air mass flow rate, kg/s
P_t = local (at the depicted cross location) total pressure in inlet distortion tests, cf. LDC
p = roll rate, rad/s
q = pitch rate, rad/s
$\bar{q}$ = dynamic pressure, employed with reference area s, $(\frac{1}{2})\rho v^2$, N/m²
Re = Reynolds number, dimensionless

Received Feb. 3, 1992; revision received May 15, 1992; accepted for publication June 2, 1992.

*Professor and Head of Laboratory, Jet Propulsion Laboratory, Faculty of Aerospace.
†Senior Engineer and Deputy Head, Jet Propulsion Laboratory, Faculty of Aerospace.

r = yaw rate, rad/s; or radius, m
s = reference aircraft surface area for dynamic pressure/force calculations, m^2
T = actual (net) thrust, [cf. Eqs. (16–18)] kgf; also temperature, K
T_i = ideal isentropic (net) thrust, [cf. Eqs. (16–18)], kgf
$T_{x,y,z}$ = thrust-vectored components in the (body axis) x-, y-, z-coordinates, kgf
T_v = pitch-thrust vectoring component (equals T_z for x-aligned TV engines), kgf
t = time [note that time is compressed by dynamic scale factors, cf. Eqs. (20–22)], s
V = true airspeed, m/s
W = flying vehicle weight, kgf
Y = the distance from aircraft centerline to (split-type) TV nozzle centerline, m
α = angle of attack, also AoA, deg, or rad
β = angle of sideslip, deg, or rad
ΔZ_{offset} = thrust offset, vanishes for x-aligned TV-engines, m
δ_a = aileron surface deflection (may be a differential angle), deg, or rad
δ_e = elevator (stabilator) surface deflection, deg, or rad
$\delta_{\Delta e}$ = differential elevator surface deflection, deg, or rad
δr = rudder surface deflection, deg, or rad
δ_{TV} = effective deflection angle of the jet during pitch and/or yaw thrust vectoring (may be a differential angle during a TV-roll command), deg or rad
δ_v = effective pitch-thrust vectoring angle (may be a differential angle during a TV roll command), deg or rad
δ_y = effective yaw thrust vectoring angle (may be a differential angle during a PSM-yaw command), deg or rad
$\bar{\zeta}$ = average density, kg/m^3
θ = pitch angle, deg
ϕ = bank angle, deg
ψ = heading angle, deg

Introduction

THE forthcoming availability of post-stall (PST) thrust-vectored-controlled (TVC) fighters, helmet-sight-aiming systems, all-aspect missiles, and the new generation of EW systems, requires reassessment of the optimal balance between aircraft agility and effectiveness, and those of missiles. Whatever is the aforementioned balance, high-performance fighter aircraft will gradually include improved thrust-vectoring propulsion-flight-control and high beta/alpha missile-launch capability.

In offensive air-to-air engagements it translates to the ability to point the nose/weapon at the enemy first during computer/system delay times. This means the capability to exploit inherent computer system missile-release delay times, i.e., from pilot's decision-time to shoot until secure-locking missile's release-time, for simultaneous rapid nose-pointing toward the target to minimize missile's flight-path time to target.

This minimum-time rule increases kill-ratio probabilities to destroy the target prior to launching its weapon, otherwise the probabilities of mutual destruction increase dramatically. Consequently, aircraft PST agility must be well-integrated with the missile's PST agility and initial vectoring conditions.

Such new developments require reassessment of all conventional propulsion flight-control concepts including the development of a new research, development, and testing methodology for integrated propulsion and flight-control criteria. An attempt to develop such a methodology is depicted in Fig. 1 and is described below.

Vectorable Nozzles and Inlets

The methodology introduces three complementary scale methods to develop post-stall thrust vectoring (PST-TV) nozzles and inlets: 1) static "subscale" tests (Figs. 2 and 3); 2) static "full-scale" tests (Fig. 4); and 3) dynamic subscale tests by means of flying "dynamically-scaled," PST-TV-powered prototypes (cf., Fig. 5).

Being properly integrated with a new mathematical phenomenology for PST-TVC, these test levels help the new search to maximize PST-TV agility.[1–3]

A few inlet test results are depicted in Figs. 6 and 7 for a "vectorable lip subscale F-15 inlet" (Figs. 6 and 7). The data

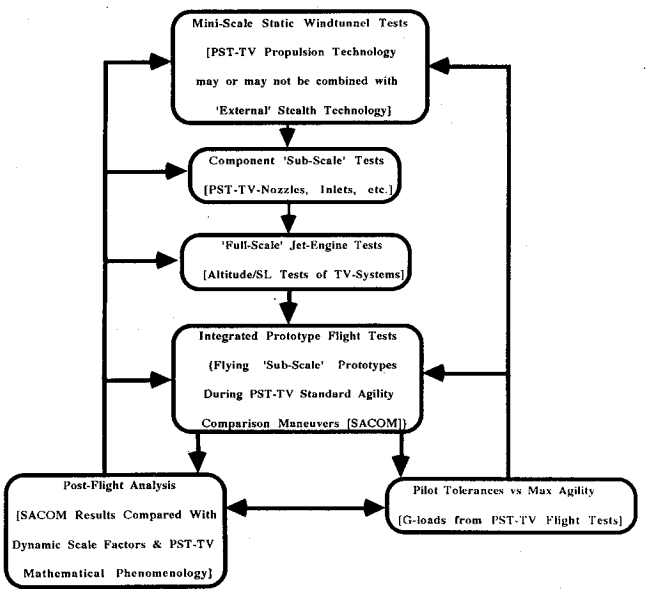

Fig. 1 Methodology developed by this laboratory.

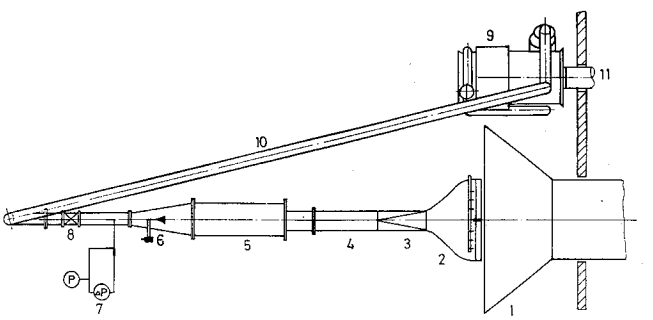

Fig. 2 Component subscale system for testing vectoring nozzles: 1) exhaust; 2) TV nozzle; 3, 4) transition–cooling sections; 5) T-56 combustor; 6) fuel injector; 7) flow monitoring; 8) flow-control valve; 9) high-pressure gas turbine; 10) connecting pipe; and 11) exhaust.

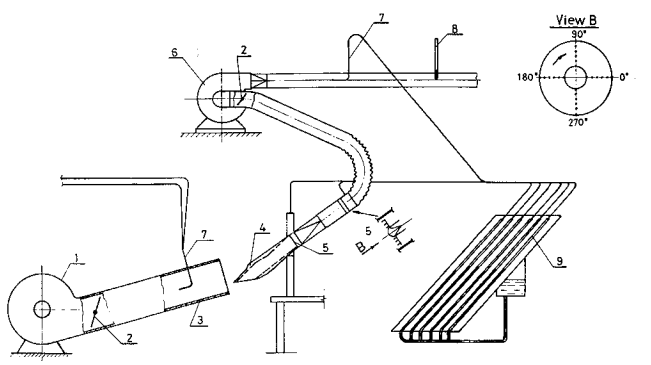

Fig. 3 Component subscale system for testing PST-inlets: 1) blowing fan; 2) airflow control; 3) duct; 4) PST-inlet with rotatable pressure probes (view B); 5) AoA control mechanism; 6) suction fan simulates engine suction; 7) uniformities monitors; 8) air temperature; and 9) multiple-tube manometers.

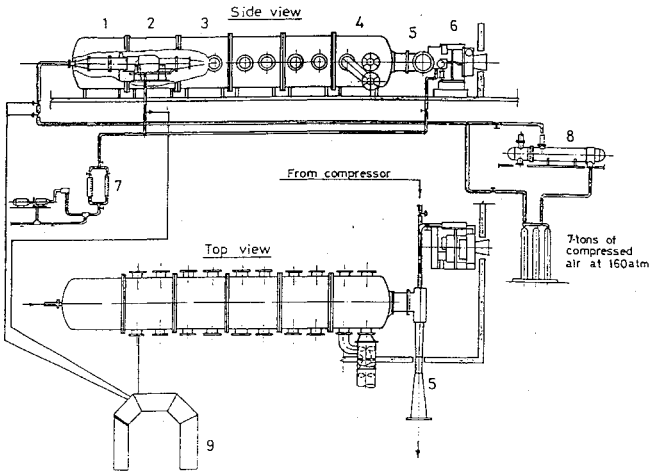

Fig. 4 Full-scale altitude jet-engine test facility: 1, 2, 3) engine sectors allow yaw-pitch nozzles for PST-TV F-15, F-16, and F-22 fighter aircraft to operate with vectorable inlets; 4, 5, 6) evacuation facilities; 7) fuel systems; 8) heat exchanger; and 9) control room.

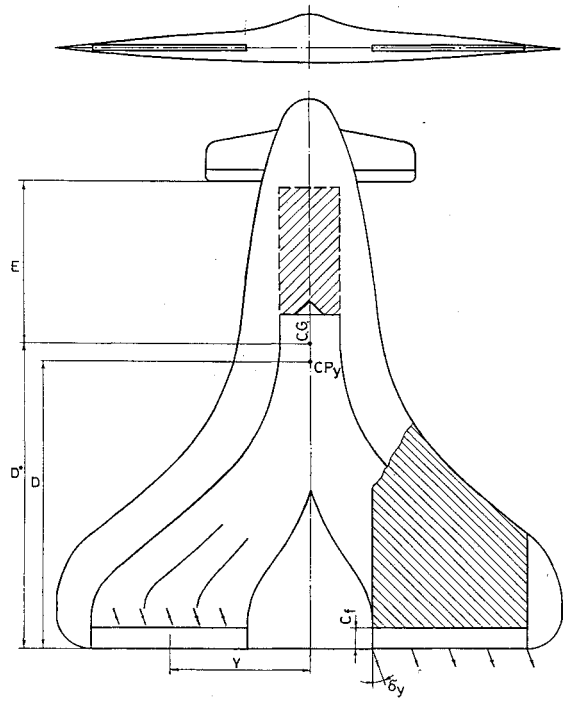

Fig. 5 First family of flying roll-yaw-pitch PST-TV prototypes. Shaded area represents super circulation-affected wing section.

indicate that a major distortion problem evolves beyond about 60 deg angle of attack (AoA), thereby demonstrating the need for inlet vectorable lips during deep PST-maneuvers.

The full-scale test rig is based on a Marbore-II engine equipped with novel yaw-pitch, or yaw-pitch-roll thrust-vectoring nozzles (Figs. 8 and 9). These are scaled-up versions of the subscale TV nozzles. The propulsion-system-scale of all our flying PST-TV prototypes corresponds to that of the subscale test facilities. Hence, dynamic vs static comparisons become "standard requirements."

Reassessment of Conventional Concepts

TVC is either "pure" or "mixed." In pure TVC, the AoA-dependent moments generated by conventional control surfaces are entirely replaced by rapidly-deflecting engine-exhaust jet(s), i.e., pure TV aircraft can deliver top PST control power rates without recourse to ailerons, flaps, elevators, and rudders, and even the vertical tail stabilizer may become redundant (Fig. 5).

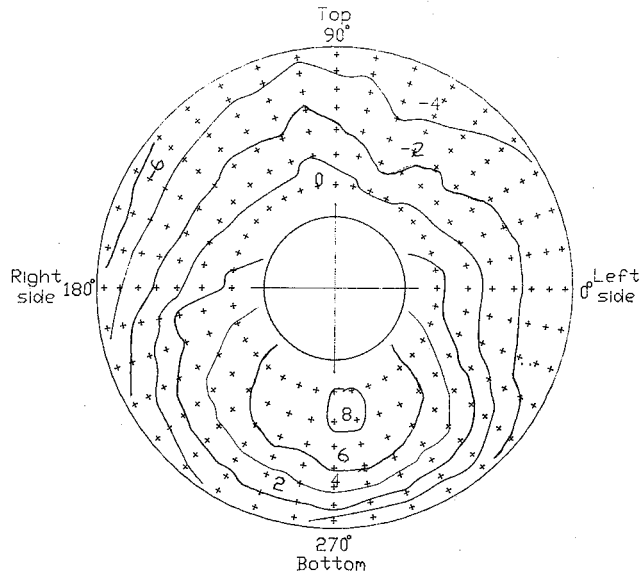

Fig. 6 Distortion generated inside inlets equipped with unvectored lips at 75-deg AoA ($\frac{1}{7}$ scale, modified F-15 inlet; LDC units; $M = 0.14$; and $Re = 10^5$).

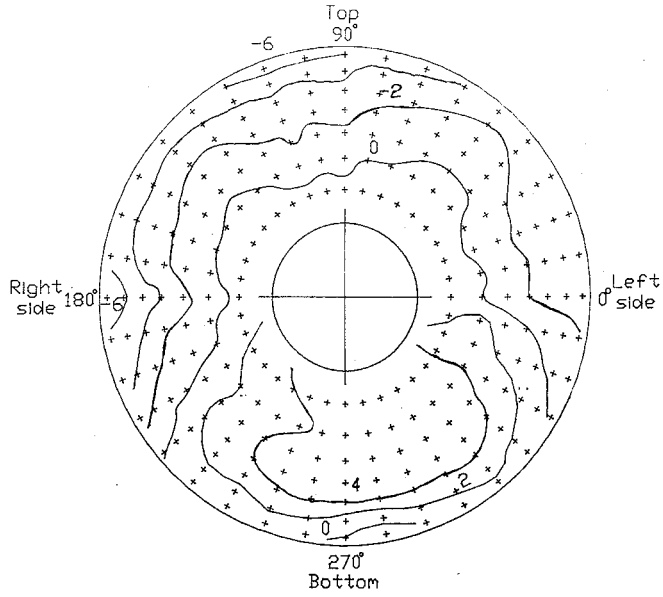

Fig. 7 50% reduction in distortion is demonstrated with inlet-lip rotated towards the incoming airflow (75-deg AoA, cf. Fig. 6).

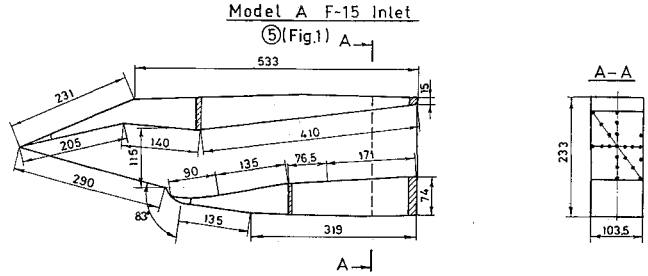

Fig. 8 Vectorable lip is rotatable to 83 deg towards the incoming airflow.

Engine forces hardly change with external-aerodynamic flow regimes, especially when equipped with PST vectorable inlets. Therefore, the control forces available for pure (thrust) vectored aircraft (PVA) remain highly effective even beyond the maximum lift AoA. Therefore, PVA present the "ideal" potential to maximize flight-control power and combat agility,[2] even in the deep PST domain. Hence, PVA concepts generate

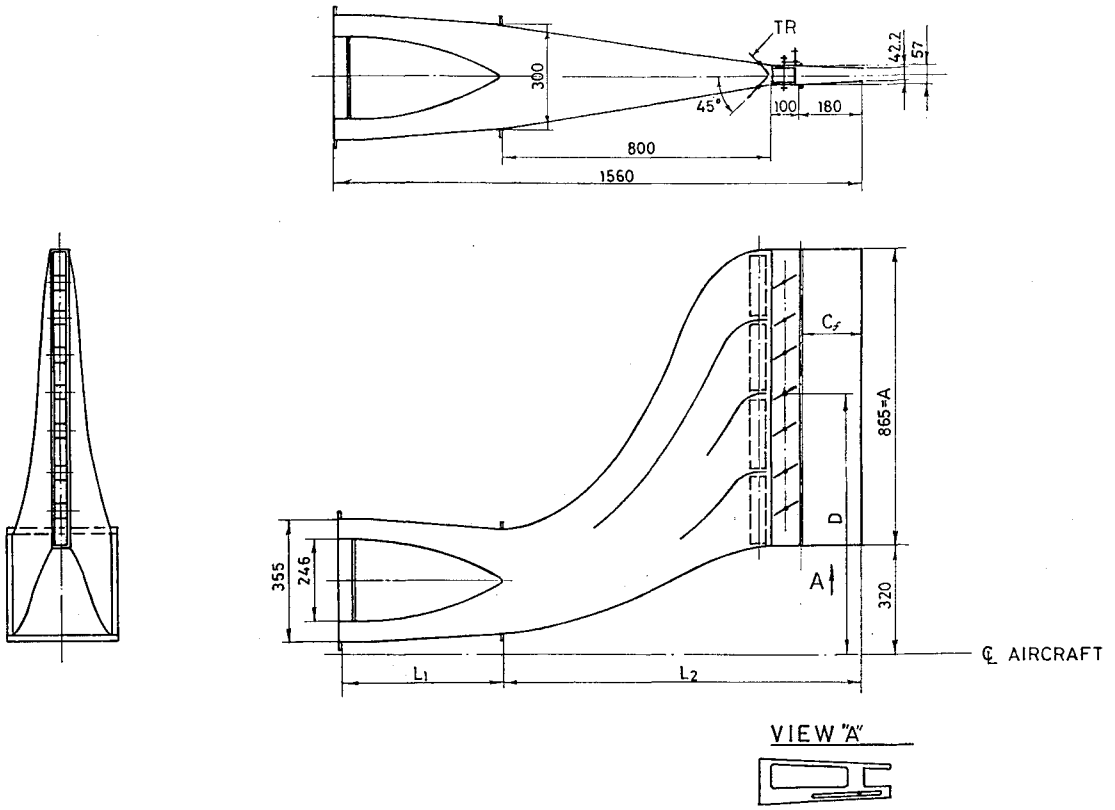

Fig. 9. Novel roll-yaw-pitch PST-TV nozzle. (Aspect ratio = 20; view "A" shows side-windows for yaw jet deflections and a simple sliding-pin mechanism for pitch TV.)

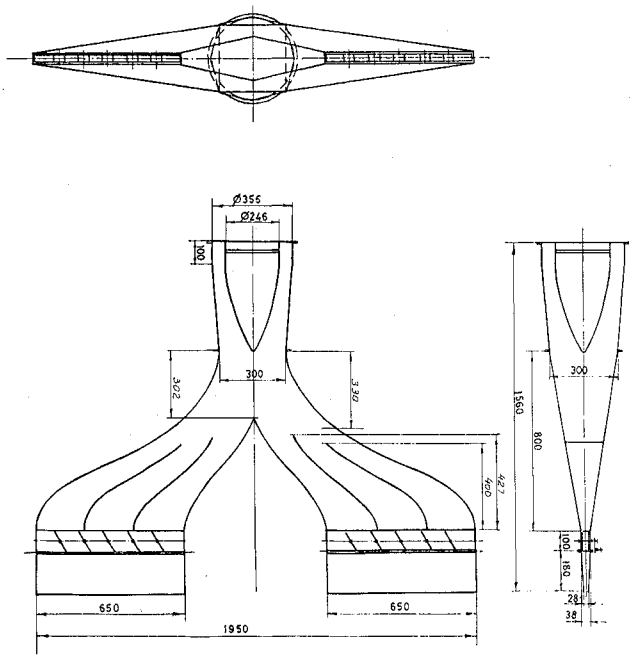

Fig. 10 Novel roll-yaw-pitch PST-TV-nozzle. (Aspect ratio = 40.)

the highest standard, or ideal reference to maximize flight control power and PST-controllability.[3]

The proposed standard has been verified recently by flight-tests involving roll-yaw-pitch TVC. The tests have demonstrated the highest payoffs at the weakest domains of conventional flight control, i.e., at low (or zero) speeds, conventionally-uncontrolled spins, very-short runways, and during rapid PST maneuvers.

Mixed TVC is employed when ailerons, elevators, and rudders are used in conjunction with TV. TVC-effectiveness must then be quantified together with the highest possible standard.

Such pure and mixed prototypes have been successfully flight-tested by this laboratory since 1987.[1-3] The yaw-pitch and roll-yaw-pitch TV nozzles employed are versions of the nozzles developed since 1983 (Figs. 5, 9 and 10). When using such powered flying models it was partially verified that there is no danger to enter into dangerous spin situations and rapid recovery is accomplished by means of a simple TV command.

Our recent flight tests also indicate that TVC can easily double or triple maximum nose turning rates.

First-Vectored Propulsion Control Rule

Whenever TVC is required the jet rotation rates should not lag behind the maximum rotation rates extractable from advanced conventional elevators, rudders, and ailerons. Therefore, effective TVC rates cannot lag behind the conventional ones. This basic effectiveness rule forces the selection of the most effective TV nozzles and TVC modes for proposed new or upgraded fighter aircraft.

To quantify and gauge this rule one must examine the time derivatives of a mathematical phenomenology for PST-TVC. This is discussed below for a few examples that have special merit in affecting future combat effectivity.

Axi-TV vs Two-Dimensional Engine Nozzles

Most axi-TV nozzle delay times result from excessive complexity and the high inertia/friction associated with a large number of moving–sliding flaps–spacers and extra rings and sliding rods–ducts (Fig. 11). The divergent flaps–spacers touch each other under maximum TV geometric deflections, thereby restricting maximum possible TV deflection angles. In comparison, there are only a few, nonsliding, rotating–deflecting flat vanes–flaps in yaw pitch two-dimensional, converging-diverging nozzles (2D-CD) nozzles. These can be rotated beyond 20 deg, and at faster rates.

Both 2D-CD and axi TV nozzles are practically similar from the combined point of view of engine reliability, performance, AB-duct design, airframe structural reinforcement, actuators-

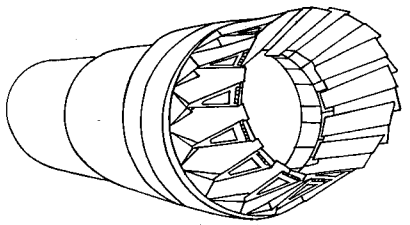

Fig. 11 Axi TV nozzles are characterized by low flight control rates.

sizes, and structure–weight–control–cost criteria required for adding TVC.

However, the internal yaw vanes of yaw-pitch 2D-CD nozzles may present extra cooling requirements of the type being currently employed for cooling advanced, first-stage, turbine stators. Provided the cooling requirements are met, the yaw-pitch TV 2D-CD nozzles must be selected by way of the previously mentioned rule.

Slow rate factors are also associated with external TV paddles of the type being flight tested now on the X-31 and F-18.

Therefore, successful criteria in air-to-air and air-to-ground TVC (or under STOL or spin-avoidance recovery conditions), include super-fast-responding yaw-pitch or yaw-pitch-roll 2D-CD TV nozzles. Consequently, such engine nozzles are being developed in this laboratory. The rest of this article examines the main theoretical parameters which affect the design of TVC systems.

Proposed Mathematical Phenomenology

Using the PVA concept a general mathematical phenomenology is constructed next for pure roll-yaw-pitch PST-TV. It defines the basic variables of pure and mixed TV aircraft and quantifies the TV control moments and rates during new combat maneuvers.

The phenomenology is characterized by the bold assumption that to describe the complex aerodynamics and rigid-body rotations–translations of advanced PST-TV-aircraft, one may still use the conventional first-order partial-derivatives of flight mechanics as an approximation. This is certainly not precise in the deep PST-domain. Hence, the phenomenology is "general" only as a pseudounified framework for treating TV terms together with conventional terms in a linearly-superimposed formulation. Consequently, the proposed unified formulation of the six degree-of-freedom equations of motion, with the yet unspecified thrust-vectoring terms, reads

$$\dot{\alpha} = q + \{-[\bar{q}sC_x/MV - (g/V)\sin\theta + r\sin\beta]\sin\alpha + [\bar{q}sC_z/MV + (g/V)\cos\theta\cos\phi - p\sin\beta]\cdot\cos\alpha\}\sec\beta \quad (1)$$

$$\dot{\beta} = -\{[\bar{q}sC_x/MV - (g/V)\sin\theta]\sin\beta + r\}\cos\alpha + [\bar{q}sC_y/MV + (g/V)\cos\theta\sin\phi]\cos\beta - \{[\bar{q}sC_z/MV + (g/V)\cos\theta\cos\phi]\cdot\sin\beta - p\}\sin\alpha \quad (2)$$

$$\dot{p} = \{-[(I_z - I_y)/I_x + I_{xz}^2/I_xI_z]qr + [1 - (I_y - I_x)/I_z]\cdot I_{xz}pq/I_x + \bar{q}sb/I_x(C_l + I_{xz}C_n/I_z)\}/(1 - I_{xz}^2/I_xI_z) \quad (3)$$

$$\dot{q} = \bar{q}scC_m/I_y + [(I_z - I_x)/I_y]pr + I_{xz}(r^2 - p^2)/I_y \quad (4)$$

$$\dot{r} = \{[I_{xz}^2/I_xI_y - (I_z - I_x)/I_z]pq - [1 + (I_z - I_y)/I_x]\cdot(I_{xz}/I_z)qr + (\bar{q}sb/I_z)[(I_{xz}/I_x)C_l + C_n]\}/(1 - I_{xz}^2/I_xI_z) \quad (5)$$

$$\dot{V}/V = [\bar{q}sC_x/MV - (g/V)\sin\theta]\cos\alpha\cos\beta + [\bar{q}sC_y/MV + (g/V)\cos\theta\sin\phi]\sin\beta + [\bar{q}sC_z/MV + (g/V)\cos\theta\cos\phi]\sin\alpha\cos\beta \quad (6)$$

$$\dot{\theta} = q\cos\phi - r\sin\phi \quad (7)$$

$$\dot{\phi} = p + r\cos\phi\tan\theta + q\sin\phi\tan\theta \quad (8)$$

$$\dot{\psi} = q\sin\phi\sec\theta + r\cos\phi\sec\theta \quad (9)$$

Unlike conventional control variables, the TVC variables hardly vary with external aerodynamic parameters such as $\bar{q}s$, α, and β. Therefore, the following division of, e.g., T_x by $\bar{q}s$, is only a matter of keeping a unified formulation with dimensionless conventional phenomenology.

Now each of the following equations contains at least one TV variable, namely

$$C_x = C_L(\alpha, \delta_e)\sin\alpha - C_D(\alpha, \delta_e)\cos\alpha\cos\beta + T_x/\bar{q}s \quad (10)$$

$$C_Y = C_Y(\alpha, |\beta|, \delta_e) + C_{Y\delta a}(\alpha)\delta_a + C_{Y\delta r}(\alpha)\delta_r + (b/2V)[C_y(\alpha)r + C_{yp}\mathrm{p}(\alpha)p] + C_{y\beta^*}(\alpha, \beta) + C_{v\delta\Delta e}(\alpha, \delta_e)\delta_{\Delta e} + T_y/\bar{q}s \quad (11)$$

$$C_z = -[C_L(\alpha, \delta_e)\cos\alpha + C_D(\alpha, \delta_e)\sin\alpha\cos\beta] + C_{(zSC)}\delta_{\mathrm{TV}} + T_v/\bar{q}s \quad (12)$$

$$C_l = C_{l\beta}(\alpha, |\beta|)\beta + C_{l\delta a}(\alpha, \delta_e)\delta_a + C_{l\delta r}(\alpha, |\delta_r|)\delta_r + (b/2V)[C_{lp}(\alpha)p + C_{lr}(\alpha)r] + C_{l\delta\Delta e}(\alpha, \delta_e)\delta_{\Delta e} + \Delta C_{l\beta}(\alpha, \beta) + C_{l\mathrm{TV}}\delta_{\mathrm{TV}} \quad (13)$$

$$C_m = C_{mo}(\alpha, \delta_e) + (c/2V)C_{mq}(\alpha)q + T(\Delta Z_{\mathrm{offset}})/\bar{q}sc + C_{mSC}\delta_{\mathrm{TV}} + C_{m\mathrm{TV}}\delta_{\mathrm{TV}} \quad (14)$$

$$C_n = C_{n\beta}(\alpha, \beta, \delta_e)\beta + C_{n\delta_a}(\alpha)\delta_a + C_{n\beta}(\alpha, \beta) + C_{n\delta r}(\alpha, \beta, \delta_r, \delta_e)\delta_r + (c/2V)[C_{np}(\alpha)p + C_{nr}(\alpha)r] + C_{n\delta\Delta e}(\alpha, \delta_{\Delta e})\delta_{\Delta e} + \Delta C_{n\beta}(\alpha, \beta) + C_{n\beta^*}(\alpha, \beta) + C_{n\mathrm{TV}}\delta_{\mathrm{TV}} \quad (15)$$

$$T_x = C_{fg}(\delta_v, \delta_y, \mathrm{NPR})T_i(M, T)\cos\delta_v\cos\delta_y \quad (16)$$

$$T_v = -C_{fg}(\delta_v, \delta_y, \mathrm{NPR})T_i(M, T)\sin\delta_v\cos\delta_y = T_z \quad (17)$$

$$T_y = C_{fg}(\delta_v, \delta_y, \mathrm{NPR})T_i(M, T)\cos\delta_v\sin\delta_y \quad (18)$$

This set of 18 equations completes our unified formulation for conventional, mixed, or pure TV flight tests.

Definitions of TV Control Terms

Roll TVC is generated by two nozzles (Fig. 7), or subnozzles (Fig. 8), each vectoring the δ_v jets in opposite directions.[4] To generate steady-state, transient sideslips, or TV-induced coupled-roll maneuvers, the δ_y jets may be deflected into different (steady-state) or similar (transient) directions.[1–4]

The δ_v and δ_y angles in Eqs. (16–18) are effective (actual) jet deflections. T_i varies with air mass flow rate and exit-gas velocity. Provided the nozzle's exit–throat area ratio is properly controlled during TV pitch and yaw deflections,[1] mass flow rate and C_{D8} values remain invariant under constant nozzle pressure ratio (dimensionless) (NPR), or constant

throttle, M and T. However, TV deflections reduce C_{D8} and C_{fg} values. Minimization of such reductions is extractable from high-aspect ratio nozzles (cf., Figs. 12 and 13). During supermaneuvers conducted with any TV nozzle and a fixed throttle as recommended[3] for conducting a rapid SACOM at approximately constant Mach and altitude

$$T_x = C_{fg}(\delta_v, \delta_y)T_i \cos \delta_v \cos \delta_y \quad (19)$$

$$T_v = C_{fg}(\delta_v, \delta_y)T_i \sin \delta_v \cos \delta_y \quad (20)$$

$$T_y = -C_{fg}(\delta_v, \delta_y)T_i \cos \delta_v \sin \delta_y \quad (21)$$

The C_m equation contains two terms associated with pitch TV: 1) $C_{mSC}\delta_{TV}$, and 2) $C_{mTV}\delta_{TV}$. The first is affected by $\bar{q}s$, whereas this effect on $C_{mTV}\delta_{TV}$ is different and less pronounced. Therefore, except for the "supercirculation" terms in Eqs. (12–14), the other TV terms are treated irrespective of $\bar{q}s$. Thus, during pure TV, the dynamic pressure term which multiplies C_m in Eq. (4) is canceled out by using proper units such as those in Eq. (12).

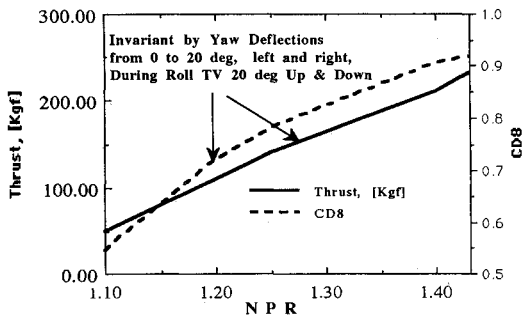

Fig. 12 C_{D8} and thrust reductions during yaw TV deflections are minimized with high-aspect ratio nozzles.

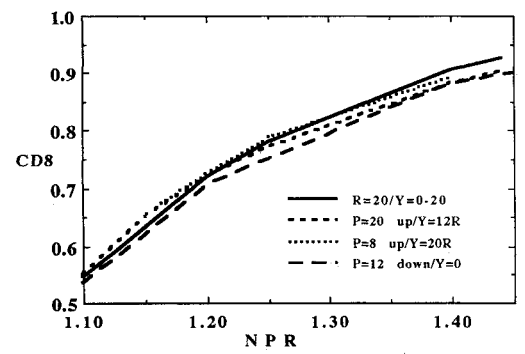

Fig. 13 Reduction in C_{D8} during TV deflections in pitch, yaw, and roll coordinates.

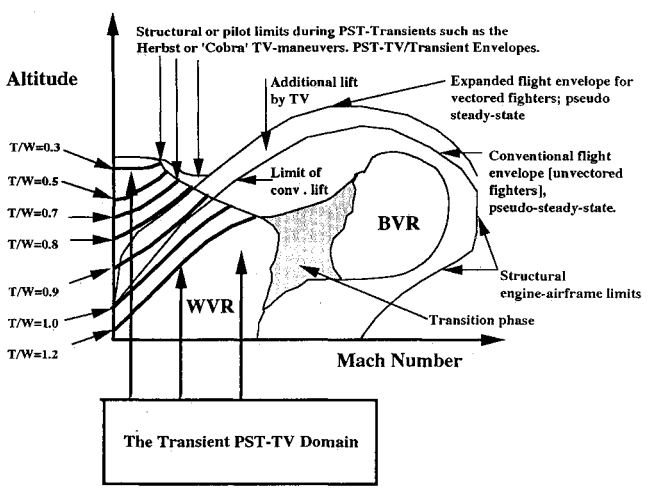

Fig. 14 Domain of PST-TV flight control.

However, only high-aspect ratio TV nozzles that are well-integrated with wing-trailing edges increase supercirculation-lift during jet-down deflections, thereby helping expanding flight envelopes (Fig. 14).

Restrictions and Approximations

Mach number effects enter the TV phenomenology through their increase of NPR and its resulting effects on thrust C_{fg} metrics. The metrics are functions of engine–aircraft–performance parameters such as inlet configuration–control mode, Mach number, altitude, AoA, sideslip angle, throttle, and nozzle configuration and control modes.[1]

Only low-speed maneuvers are analyzed next, i.e., for $M < 0.4$–0.6. Hence, the PST-TV maneuvers are assumed to be conducted in the incompressible flow regime. Various other effects have been neglected in this model. For instance, asymmetric and inertia effects due to fuel distribution and sloshing, or elasticity–relaxation phenomena and air-turbulence noise. Moreover, during very rapid rigid body dynamics-controlled "flip-up–down" or "rotational-whippings" of the nose–bottom of the aircraft, the induced inertia–gyroscopic effects play much higher roles than with relatively sluggish conventional fighter aircraft.

To maximize the highly required PST-TV roll moment and rates, the length of the TV-rolling arm Y must be maximized–optimized. Similar conclusions apply to D and D^*.

Agility and Dynamic Scaling

With the rapid advancement of new technologies, engagement times get shorter, and the minimization of inherent delay times of TV nozzles, pilot, and thrust-vectoring control-integrated flight propulsion control (TVC-IFPC) hardware become more critical to combat effectiveness. Hence, to simulate TV controllability by flying powered-scaled models, we define aircraft gross agility (AGA) as

$$\text{AGA} = \text{MGA(DSF)}F_1(\text{Turb.} - \text{MLEM})F_2(\text{PDT/FDT}) \cdot F_3(A - \text{IFPC})/(M - \text{IFPC}) \quad (22)$$

where MGA is the scaled model gross agility, DSF the dynamic scale factors (to be defined below), F_1(Turb. – MLEM) the functions of turbulence noise and maximum likelihood estimation method, F_2(PDT/FDT) the ratio of pilot to flyer delay times during actual in-flight standard agility comparison maneuver(s) (SACOM), and $F_3(A - \text{IFPC})/(M - \text{IFPC})$ the control functions relating aircraft IFPC to model-IFPC. Without stating it, Eq. (22) assumes that each vehicle is characterized by a hidden bona fide net agility, a basic combat-technological quality that the propulsion–airframe designer and the theoretician both want to uncover and continuously maximize.

One assumes that differences in aerodynamic effects between model and full-scale aircraft are of "second-order" in comparison with moments-of-inertia related angular velocities and accelerations. This approximation is justified especially for high Re number ranges and for a strict proportional size-shape similarity between the full-scale aircraft and scaled models. Therefore

$$(\mathrm{d}x_i)_A/(\mathrm{d}x_i)_M = L \qquad (i = 1, 2, 3, \text{ or } x, y, z);$$

$$r_A = Lr_M \quad (23)$$

$$W_M = Mg \cong g\bar{\zeta}_M \int_{V_M} (\mathrm{d}x_i)_M = g\bar{\zeta}_M L^{-3} \int_{V_A} (\mathrm{d}x_i)_A$$

$$= W_A L^{-3}(\bar{\zeta}_M/\bar{\zeta}_A) \quad (24)$$

$$I_M = \int_{M_M} r_M^2 \, dM_M \cong \bar{\zeta}_M \int_{V_A} L^{-2} r_A^2 L^{-3} \, (dx_i)_A$$

$$= \bar{\zeta}_M L^{-5} \int_{V_A} r_A^2 \, (dx_i)_A = I_A(\bar{\zeta}_M/\bar{\zeta}_A)L^{-5} \tag{25}$$

where

$$\int_{V_A} r_A^2 \, (dx_i)_A \cong I_A/\bar{\zeta}_A \tag{26}$$

and M is mass, W weight, r radius, and the subscripts M and A refer to model and full-scale aircraft, respectively, while $\bar{\zeta}$ is the average density and L the linear-scale factor.

For MGA angular reversal rates (ARR), for pitch, roll, and yaw rate reversals we write

$$\text{AGA(ARR)} = \text{MGA(ARR)(L)}^{-0.5} F_2(\text{Turb.} - \text{MLEM})$$

$$\cdot F_2(\text{PDT/FDT}) F_3(A - \text{IFPC})/(M - \text{IFPC})$$

$$\cong \text{MGA(ARR)}(L)^{-0.5} \tag{27}$$

where as a first iteration the functionals $F_1F_2F_3$ are approximated by unity, aircraft performance angles remain scale invariants, and (agility) time is compressed by the factor $(L)^{-0.5}$.

The maximum (gross) pitch rate observed so far with our $\frac{1}{7}$ scale flying PST-TV F-15 model is around 200 deg/s. By 27, it is around $(200)(7)^{-0.5}$ for the full-scale F-15 (i.e., around three times the current maximum rate).

The errors involved in using such dynamic scale factors do not depend on any assumption related to the model or full-scale Reynolds or Froude numbers. Equations (24, 25, and 27) are therefore based on simple physical laws irrespective of any boundary-layer assumptions. Recent laboratory and flight-testing verifications of these equations provide verification of this methodology.

Approximate Phenomenology for Comparative Studies

During rapid cobra-type maneuvers (Figs. 15 and 16), the vehicle is rapidly "whipping" the air. This rapid nose-pointing reversal keeps the vehicle's flight-path approximately horizontal for a short duration. Depending on its T/W, stability margin, IFPC–flyer-delay times, Mach number, altitude, and SACOM duration, the vehicle may gain altitude prior to reversing this trend during a positive cobra maneuver, while the flight-path is consistently downward during a negative cobra maneuver.

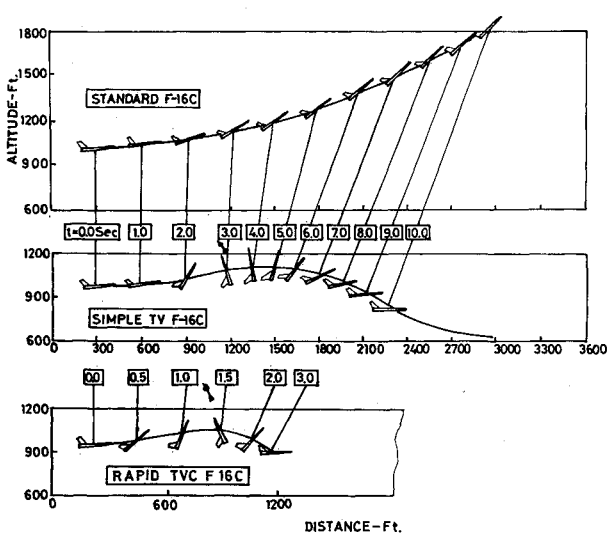

Fig. 15 Rule 1: Maximum jet-vectoring rates should equal conventional deflection rates. Upper figure, conventional turning rate at maximum pilot tolerance and restricted maximum AoA. Lower figure, at low speeds, the faster the maneuver, the safer it becomes for a pilot located near the center of rotation. Midfigure, slow PST-TV-induced turning rate is less combat effective.

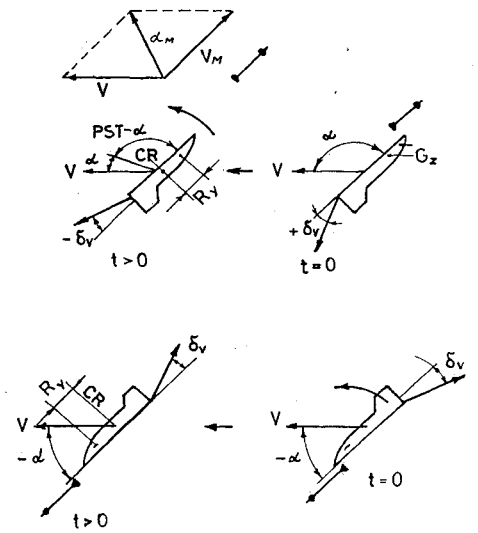

Fig. 16 Rule 2: Maximization of TV moments and rates at the reversal point of positive and negative cobra maneuvers. (Note dangerous interactions with high AoA-launched missiles. V_M = missile's initial velocity vector whose magnitude increases with launch rail length.)

The low ratio of altitude change to the horizontal distance covered during very rapid maneuvers allows one to assume that as a SACOM-approximation the flight path remains at a "pseudoconstant-altitude."

Under these conditions, ϕ, β, $\dot{p}$, p, $\dot{r}$, r, $\dot{\beta}$, δ_e, δ_a, δ_r, $\delta_{\Delta e}$, C_l, C_n, and C_Y vanish, while $\theta \cong \alpha$ and $\dot{\alpha} \cong q$. Moreover, the supercirculation term can be neglected for the low-aspect ratio TV nozzles of our early PST-TV F-15 flying models. The term $T(\Delta Z_{\text{offset}})$ vanishes when the thrust acts through CG, as is the case with all our scaled TV vehicles. Under these conditions the flyer command is pure δ_v-input, for which

$$C_x = C_L(\alpha)\sin\alpha - C_D(\alpha)\cos\alpha + T_x/\bar{q}s \tag{28}$$

$$C_Y = 0 \tag{29}$$

$$C_z = -[C_L(\alpha)\cos\alpha + C_D(\alpha)\sin\alpha] + T_v/\bar{q}s \tag{30}$$

$$C_l = 0 \tag{31}$$

$$C_m = C_{mo}(\alpha) + C_{m\text{TV}} \cdot \delta_v + (C/2V)C_{mq}(\alpha)q \tag{32}$$

$$C_n = 0 \tag{33}$$

$$Mg = \bar{q}s(C_x \sin\alpha - C_z \cos\alpha) \tag{34}$$

$$\dot{q}I_y = \bar{q}sc[C_{mo}(\alpha) + (C/2V)C_{mq}(\alpha)q + C_{m\text{TV}} \cdot \delta_v] \tag{35}$$

$$M\dot{V} = \bar{q}s(C_x \sin\alpha + C_z \cos\alpha) \tag{36}$$

During this SACOM 19–21 are reduced to

$$T_x = C_{fg}(\delta_v)T_i \cos\delta_v \tag{37}$$

$$T_v = -C_{fg}(\delta_v)T_i \sin\delta_v \tag{38}$$

$$T_y = 0 \tag{39}$$

Equations (28–39) are employed to generate a practical SACOM, starting from steady-level flight conditions and ending at similar conditions.[3]

Numerical and analytical solutions of this set (with particular initial and boundary conditions) can be investigated while working back and forth between theory and well-controlled SACOM. The tests can verify the variation of q, $\dot{q}$, and $\ddot{q}$ with the time-variations and range of the δ_v command at different true air speeds. For this purpose we instrument the

dynamically-scaled models with three gyros, three accelerometers, and α, β, and V probes. During the SACOM each variable is recorded 20 times/s on an onboard computer. A synchronized ground computer simultaneously records 40 times/s the conventional and/or the TV commands.

90-Deg AoA Reversals

This variant is defined by TV commands which reverse the jet direction at exactly positive or negative 90-deg AoA, namely, when the aerodynamic "lift" vanishes. This reduces Eqs. (28–39) to

$$C_x = [C_{fg}(\delta_v)T_i \cos \delta_v]/\bar{q}s \tag{40}$$

$$C_z = [-C_D(90) + C_{fg}(\delta_v)T_i \sin \delta_v]/\bar{q}s \tag{41}$$

$$C_m = C_{mo}(90) + C_{m\mathrm{TV}} \cdot \delta_v \tag{42}$$

$$M''g'' = C_{fg}(\delta_v)T_i \cos \delta_v \tag{43}$$

$$\dot{q}I_y = D^* C_{fg}(\delta_v)T_i \sin \delta_v \tag{44}$$

$$M\dot{V} = C_{fg}(\delta_v)T_i \cos \delta_v = T_x \tag{45}$$

Thus, for this readily measurable SACOM $q \cong 0$ and

$$\dot{q} \propto C_{fg}(\delta_v)\sin \delta_v \tag{46}$$

Analytical integrations and differentiations of Eqs. (44) and (45) with various IFPC–flyer delay times are readily derived for a Dirac-type or other step-function TV time commands.

Forbidden Human Space-Time Domains

Situating an hypothetical pilot's head at *CR*—the center of rotation (where there are no centrifugal and tangential accelerations during rapid pure pitch-up/down cobra whippings), the normal acceleration on his head is roughly approximated by

$$G_z = \{\bar{q}s[C_L(\alpha)\cos \alpha + C_D(\alpha)\sin \alpha] - T_v\}/M \tag{47}$$

or, for the simplifying 90-deg AoA pitch SACOM reversal (when δ_v changes sign), by

$$G_z = [\bar{q}sC_D(90) + C_{fg}(\delta_v)T_i \sin \delta_v]/M \tag{48}$$

G_z does not change sign when δ_v does (Fig. 16). The hypothetical pilot starts sensing "negative-g" (blood flow into brain) only when at low speed–drag values

$$[-T_v + \bar{q}sC_D(90)] < 0 \tag{49}$$

More generally, speed reduction due to $\bar{q}s[C_L(\alpha)\cos \alpha + C_D(\alpha)\sin \alpha]$ acts to defer crossing into negative-g domains, for it introduces a compensating "positive-g" component (blood flow from brain). Situating the pilot ahead of *CR* adds positive or negative tangential pitch acceleration and allows simple calculations of total G_z for a realistic pilot.

Consequently, crossing into negative-g domains depends on AoA, airspeed, pilot's distance from *CR*, q, and the value, sign, and duration of the command.

G_x includes positive (blood flow to chest) "centrifugal" acceleration acting on the pilot. The noncentrifugal/rotational component of G_x (when the hypothetical pilot is situated at *CR*) is roughly approximated by

$$G_x = \{\bar{q}s[-C_L(\alpha)\sin \alpha + C_D(\alpha)\cos \alpha] - T_x\}/M \tag{50}$$

Similarly, the noncentrifugal/rotational portions of G_x and G_y can be measured and compared with load approximations for PSM

$$G_x = \{-C_{fg}(\delta_y)T_i \cos \delta_y + \bar{q}sC_D[\alpha(0)]\}/M \tag{51}$$

$$G_y = [-\bar{q}sC_y(\beta) - C_{fg}(\delta_y)T_i \sin \delta_y]/M \tag{52}$$

The G_z, G_y, and G_x pilot tolerances vary differently with the duration and rate of onsets. Therefore, combined with such (a priori known) duration–rate limitations, the measurement envelopes translate into forbidden human space-time agility domains of supermaneuvers.

These domains have not yet been explored. Their boundaries vary, inter alia, with the distance from the pilot's head to the so-called pseudoinstantaneous center-of-rotation during different rapid supermaneuvers. Understanding these complex rigid-body translational, rotational, gyration, and gyroscopic phenomena, requires reassessment of well-established concepts.

Concluding Remarks

Fundamental concepts of vectored propulsion have been defined and represented by novel designs of TV-nozzles for maximized PST-agility. These concepts have been employed to formulate a unified mathematical phenomenology of PST-vectored fighter aircraft.

The phenomenology has been combined with an unorthodox methodology to test alternative prototypes of agile tailless vectored fighters and the efficiency of upgraded (conventional) fighters. Two PST-TV control rules have also been formulated.

Acknowledgments

Part of this research has been financially sponsored by the U.S. Air Force Office of Scientific Research, EOARD, U.K., General Dynamics, General Electric, Teledyne, and Pratt and Whitney. We thank the following individuals for encouraging and trusting us with an unorthodox research work: G. Keith Richey, Douglass Bowers, T. Speers, W. Lindsay, J. Wigle, W. Calarese, John Tedor, Daniel W. Repperger, and Daniel Baumann, all from the USAF; Ben Koff, R. E. (Bob) Davis, Jeffery Schweitzer, and J. Cahill, from PWA; Eli Benstein from Teledyne CAE; J. Roug, Don Dunbar, and F. Ehric from General Electric; T. P. McAtee from General Dynamics, and the late W. B. Herbst of MBB, a pioneer and a great contributor to the recent advances of fighter aircraft supermaneuverability.

References

[1]Gal-Or, B., *Vectored Propulsion, Supermaneuverability and Robot Aircraft*, Springer-Verlag, New York, 1990, 1991.

[2]Gal-Or, B., "The Fundamental Concepts of Vectored Propulsion," *Journal of Propulsion and Power*, Vol. 6, No. 6, 1990, pp. 747–757.

[3]Gal-Or, B., "Maximizing Post-Stall, Thrust-Vectoring Agility and Control Power," *Journal of Aircraft* (to be published).

[4]Gal-Or, B., *Flight-Control for Jet-Propelled Aircraft and Spacecraft*, Patent Appl. 80532, 7.11.86, Israel.